

# The Steklov spectrum of the Helmholtz operator

Kshitij Patil, Nilima Nigam

Department of Mathematics  
Simon Fraser University

Algoritmy March 16, 2024

# The Steklov-Helmholtz eigenvalue problem

[see applications](#)

Let  $\Omega \subset \mathbb{R}^2$  be bounded.

The **Steklov-Helmholtz EVP**

(Steklov, 1895) for fixed real wave number  $\mu$  is to find:  $\sigma \in \mathbb{R}$  and  $u$  such that

$$\begin{cases} -\Delta u - \mu^2 u = 0 & \text{in } \Omega, \\ \partial_\nu u = \sigma u & \text{on } M. \end{cases}$$

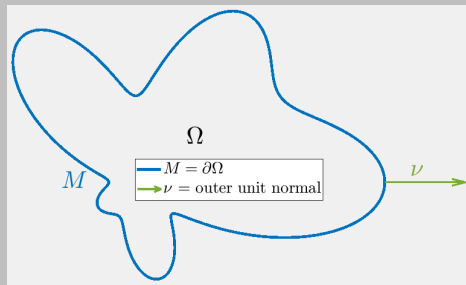


Figure 1:  $M$  is smooth enough

# The Steklov-Helmholtz eigenvalue problem

[see applications](#)

Let  $\Omega \subset \mathbb{R}^2$  be bounded.

The **Steklov-Helmholtz EVP**

(Steklov, 1895) for fixed real wave number  $\mu$  is to find:  $\sigma \in \mathbb{R}$  and  $u$  such that

$$\begin{cases} -\Delta u - \mu^2 u = 0 & \text{in } \Omega, \\ \partial_\nu u = \sigma u & \text{on } M. \end{cases}$$

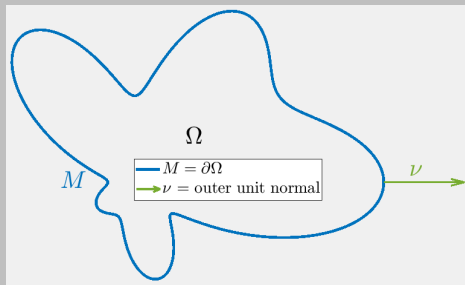


Figure 1:  $M$  is smooth enough

Informally, if  $\mu^2 \rightarrow$  Dirichlet-Laplace eigenvalue, then  $\sigma \rightarrow -\infty$ .

# Literature Survey: Steklov-Laplace

Topic		Reference
Review		(Kuznetsov et al., 2014), (Girouard and Polterovich, 2017)
Eigenvalue bounds		(WEINSTOCK, 1954), (Hersch et al., 1974), (Girouard and Polterovich, 2010)
Asymptotics		(Girouard, Karpukhin, et al., 2021), (Levitin et al., 2022) (sec. 7.2.1, 7.3.1)
Isoperimetric inequalities		(Fraser et al., 2009), (Fraser et al., 2012)
Shape optimization		(Caubet et al., 2022), (Akhmetgaliyev, Kao, et al., 2017), (Alhejaili et al., 2019), (Antunes, 2021), (Oudet et al., 2021)
Extrinsic shape analysis		(Wang et al., 2018)
Layer potentials		(Imeri et al., 2022)

**Table 1:** Some of the literature on the Steklov-Laplace eigenvalue problem.

# Literature Survey: Steklov-Helmholtz

Topic		Reference
Review		(Levitin et al., 2022) (sec. 7.4)
Modified Helmholtz problem		(Tang et al., 1998), (Huang et al., 2004), (Turk, 2021)
Non self-adjoint problem		(Arendt et al., 2012), (Meng et al., 2020)
Inverse scattering		(Cakoni, Colton, et al., 2016)
Layer potentials		(Ma et al., 2022)

Table 2: Some of the literature on the Steklov-Helmholtz eigenvalue problem.

## Contributions

see curves

We suggest an exponentially converging numerical scheme to approximate the **Steklov-Helmholtz EVP**. We have

- a homothety result,
- conjectures about the number of negative eigenvalues and the asymptotic behaviour of the spectrum.

Can be adapted to other EVPs such as the **Dirichlet/Neumann/Robin-Laplace EVPs** and the **transmission EVP**.

MATLAB code.

## The Helmholtz equation (Colton et al., 2013)

[properties](#)

For a fixed real wave number  $\mu \in \mathbb{R}$ , recall the Helmholtz equation:

$$-\Delta u - \mu^2 u = 0.$$

The fundamental solution of the Helmholtz equation is the function:

$$G_\mu(x, y) := \frac{i}{4} H_0^1(\mu|x - y|), \quad x \neq y,$$

where  $H_0^1$  is the Hankel function of the 1st kind and order 0.

$H_0^1$  has a logarithm singularity at  $x = y$ .

## Layer Potentials (Colton et al., 1983), (McLean, 2000)

- The single-layer potential with density  $\phi$  solves the Helmholtz equation,

$$[\mathcal{S}_{\mu}\phi](x) = 2 \int_M \phi(y) G_{\mu}(x, y) ds_y, \quad x \in \mathbb{R}^2 \setminus M.$$

## Layer Potentials (Colton et al., 1983), (McLean, 2000)

- The single-layer potential with density  $\phi$  solves the Helmholtz equation,

$$[\mathcal{S}_\mu \phi](x) = 2 \int_M \phi(y) G_\mu(x, y) ds_y, \quad x \in \mathbb{R}^2 \setminus M.$$

- We seek eigenfunctions  $u(x) = \frac{1}{2}[\mathcal{S}_\mu \phi](x)$ .

## Layer Potentials (Colton et al., 1983), (McLean, 2000)

- The single-layer potential with density  $\phi$  solves the Helmholtz equation,

$$[\mathcal{S}_\mu \phi](x) = 2 \int_M \phi(y) G_\mu(x, y) ds_y, \quad x \in \mathbb{R}^2 \setminus M.$$

- We seek eigenfunctions  $u(x) = \frac{1}{2}[\mathcal{S}_\mu \phi](x)$ .
- Approaching  $M$  from inside  $\Omega$ , we get the operators:

$$([\mathcal{S}_\mu \phi](x))|_M = 2 \int_M \phi(y) G_\mu(x, y) ds_y =: \tilde{S}_\mu \phi(x), \quad x \in M, \text{ and}$$

$$(\partial_\nu [\mathcal{S}_\mu \phi](x))|_M = 2 \int_M \partial_{\nu_x} G_\mu(x, y) \phi(y) ds_y + \phi(x) =: K'_\mu \phi(x) + \phi(x), \quad x \in M,$$

where  $\tilde{S}_\mu : H^{s-1/2}(M) \rightarrow H^{s+1/2}(M)$  and  $K'_\mu : H^{s-1/2}(M) \rightarrow H^{s-1/2}(M)$ .

## Layer Potentials (Colton et al., 1983), (McLean, 2000)

- The single-layer potential with density  $\phi$  solves the Helmholtz equation,

$$[\mathcal{S}_\mu \phi](x) = 2 \int_M \phi(y) G_\mu(x, y) ds_y, \quad x \in \mathbb{R}^2 \setminus M.$$

- We seek eigenfunctions  $u(x) = \frac{1}{2}[\mathcal{S}_\mu \phi](x)$ .
- Approaching  $M$  from inside  $\Omega$ , we get the operators:

$$([\mathcal{S}_\mu \phi](x))|_M = 2 \int_M \phi(y) G_\mu(x, y) ds_y =: \tilde{S}_\mu \phi(x), \quad x \in M, \text{ and}$$

$$(\partial_\nu [\mathcal{S}_\mu \phi](x))|_M = 2 \int_M \partial_{\nu_x} G_\mu(x, y) \phi(y) ds_y + \phi(x) =: K'_\mu \phi(x) + \phi(x), \quad x \in M,$$

where  $\tilde{S}_\mu : H^{s-1/2}(M) \rightarrow H^{s+1/2}(M)$  and  $K'_\mu : H^{s-1/2}(M) \rightarrow H^{s-1/2}(M)$ .

These operators are known to be continuous for sufficiently smooth  $C^{r+1,1}$   $M$ , where  $r \in \mathbb{N}_0$  and  $|s| \leq r + 1$ . [see maps](#) [see spaces](#)

# Connection to the Dirichlet to Neumann map (Cakoni and Kress, 2017),(Levitin et al., 2022)

- Our approach: PDE → BIE, discretize, solve a generalized EVP.

# Connection to the Dirichlet to Neumann map

(Cakoni and Kress, 2017),(Levitin et al., 2022)

- Our approach: PDE → BIE, discretize, solve a generalized EVP.
- The **Dirichlet to Neumann** ( $D_\mu$ ) map relates Dirichlet and Neumann traces.

# Connection to the Dirichlet to Neumann map

(Cakoni and Kress, 2017), (Levitin et al., 2022)

- Our approach: PDE → BIE, discretize, solve a generalized EVP.
- The **Dirichlet to Neumann** (DtN,  $\mathcal{D}_\mu$ ) map relates Dirichlet and Neumann traces.
- Let  $U$  solve the Helmholtz equation and  $(\mu_D^2, U_D)$  be a Dirichlet eigenpair.

$$\begin{aligned}\mu_D^2(U, U_D)_{L^2(\Omega)} &= (U, -\Delta U_D)_{L^2(\Omega)} + (u, T\partial_\nu U_D)_{L^2(M)} \\ &= \mu_D^2(U, U_D)_{L^2(\Omega)} + (u, T\partial_\nu U_D)_{L^2(M)}.\end{aligned}$$

# Connection to the Dirichlet to Neumann map

(Cakoni and Kress, 2017), (Levitin et al., 2022)

- Our approach: PDE → BIE, discretize, solve a generalized EVP.
- The **Dirichlet to Neumann** (DtN,  $\mathcal{D}_\mu$ ) map relates Dirichlet and Neumann traces.
- Let  $U$  solve the Helmholtz equation and  $(\mu_D^2, U_D)$  be a Dirichlet eigenpair.

$$\begin{aligned}\mu_D^2(U, U_D)_{L^2(\Omega)} &= (U, -\Delta U_D)_{L^2(\Omega)} + (u, T\partial_\nu U_D)_{L^2(M)} \\ &= \mu_D^2(U, U_D)_{L^2(\Omega)} + (u, T\partial_\nu U_D)_{L^2(M)}.\end{aligned}$$

- Let  $\mathcal{K}_{\mu_D}$  be the set of Neumann traces of  $U_D$ .

$$\text{dom}(\mathcal{D}_\mu) := \begin{cases} H^{1/2}(M) & \mu \neq \mu_D, \\ H^{1/2}(M) \cap \mathcal{K}_{\mu_D}^\perp & \mu = \mu_D. \end{cases}$$

# Connection to the Dirichlet to Neumann map

(Cakoni and Kress, 2017), (Levitin et al., 2022)

- Our approach: PDE → BIE, discretize, solve a generalized EVP.
- The **Dirichlet to Neumann** (DtN,  $\mathcal{D}_\mu$ ) map relates Dirichlet and Neumann traces.
- Let  $U$  solve the Helmholtz equation and  $(\mu_D^2, U_D)$  be a Dirichlet eigenpair.

$$\begin{aligned}\mu_D^2(U, U_D)_{L^2(\Omega)} &= (U, -\Delta U_D)_{L^2(\Omega)} + (u, T\partial_\nu U_D)_{L^2(M)} \\ &= \mu_D^2(U, U_D)_{L^2(\Omega)} + (u, T\partial_\nu U_D)_{L^2(M)}.\end{aligned}$$

- Let  $\mathcal{K}_{\mu_D}$  be the set of Neumann traces of  $U_D$ .

$$\text{dom}(\mathcal{D}_\mu) := \begin{cases} H^{1/2}(M) & \mu \neq \mu_D, \\ H^{1/2}(M) \cap \mathcal{K}_{\mu_D}^\perp & \mu = \mu_D. \end{cases}$$

- $\mathcal{D}_\mu : \text{dom}(\mathcal{D}_\mu) \rightarrow H^{-1/2}(M)$ ,  $\mathcal{D}_\mu \phi = (K'_\mu + I)\tilde{S}_\mu^{-1}\phi$ .
- The Helmholtz DtN map and the Steklov- Helmholtz EVP are isospectral.
- For a Lipschitz boundary  $M$ , the spectrum is discrete (real for real  $\mu$ ).

# Reformulation of Steklov-Helmholtz EVP

The boundary condition of the Steklov EVP leads to a boundary integral equation,

# Reformulation of Steklov-Helmholtz EVP

The boundary condition of the Steklov EVP leads to a boundary integral equation,

$$\underbrace{\int_M \partial_{\nu_x} G_{\mu}(x, y) \phi(y) ds_y + \frac{\phi(x)}{2}}_{(K'_{\mu} \phi + \phi)/2} = \sigma \underbrace{\int_M G_{\mu}(x, y) \phi(y) ds_y}_{(\tilde{S}_{\mu} \phi)/2}.$$

# Reformulation of Steklov-Helmholtz EVP

The boundary condition of the Steklov EVP leads to a boundary integral equation,

$$\underbrace{\int_M \partial_{\nu_x} G_{\mu}(x, y) \phi(y) ds_y + \frac{\phi(x)}{2}}_{(K'_{\mu} \phi + \phi)/2} = \sigma \underbrace{\int_M G_{\mu}(x, y) \phi(y) ds_y}_{(\tilde{S}_{\mu} \phi)/2}.$$

Let  $z(t)$ ,  $t \in [0, 2\pi]$ , where  $|z'(t)| > 0$  for all  $t$  be a smooth  $2\pi$  periodic boundary parameterization.

# Reformulation of Steklov-Helmholtz EVP

The boundary condition of the Steklov EVP leads to a boundary integral equation,

$$\underbrace{\int_M \partial_{\nu_x} G_{\mu}(x, y) \phi(y) ds_y + \frac{\phi(x)}{2}}_{(K'_{\mu} \phi + \phi)/2} = \sigma \underbrace{\int_M G_{\mu}(x, y) \phi(y) ds_y}_{(\tilde{S}_{\mu} \phi)/2}.$$

Let  $z(t)$ ,  $t \in [0, 2\pi]$ , where  $|z'(t)| > 0$  for all  $t$  be a smooth  $2\pi$  periodic boundary parameterization.

$$\int_0^{2\pi} L(t, \tau) \psi(\tau) d\tau + \psi(t) = \sigma \int_0^{2\pi} M(t, \tau) \psi(\tau) d\tau,$$

where the kernels  $L, M$  depend on  $\mu$  and have logarithmic singularities when  $t = \tau$ . [see kernels](#)

# Reformulation of Steklov-Helmholtz EVP

The boundary condition of the Steklov EVP leads to a boundary integral equation,

$$\underbrace{\int_M \partial_{\nu_x} G_{\mu}(x, y) \phi(y) ds_y + \frac{\phi(x)}{2}}_{(K'_{\mu} \phi + \phi)/2} = \sigma \underbrace{\int_M G_{\mu}(x, y) \phi(y) ds_y}_{(\tilde{S}_{\mu} \phi)/2}.$$

Let  $z(t)$ ,  $t \in [0, 2\pi]$ , where  $|z'(t)| > 0$  for all  $t$  be a smooth  $2\pi$  periodic boundary parameterization.

$$\int_0^{2\pi} L(t, \tau) \psi(\tau) d\tau + \psi(t) = \sigma \int_0^{2\pi} M(t, \tau) \psi(\tau) d\tau,$$

where the kernels  $L, M$  depend on  $\mu$  and have logarithmic singularities when  $t = \tau$ . [see kernels](#)

We find eigendensities  $\psi$  and eigenvalues  $\sigma \in \mathbb{R}$ .

# Reformulation of Steklov-Helmholtz EVP

The boundary condition of the Steklov EVP leads to a boundary integral equation,

$$\underbrace{\int_M \partial_{\nu_x} G_{\mu}(x, y) \phi(y) ds_y + \frac{\phi(x)}{2}}_{(K'_{\mu} \phi + \phi)/2} = \sigma \underbrace{\int_M G_{\mu}(x, y) \phi(y) ds_y}_{(\tilde{S}_{\mu} \phi)/2}.$$

Let  $z(t)$ ,  $t \in [0, 2\pi]$ , where  $|z'(t)| > 0$  for all  $t$  be a smooth  $2\pi$  periodic boundary parameterization.

$$\int_0^{2\pi} L(t, \tau) \psi(\tau) d\tau + \psi(t) = \sigma \int_0^{2\pi} M(t, \tau) \psi(\tau) d\tau,$$

where the kernels  $L, M$  depend on  $\mu$  and have logarithmic singularities when  $t = \tau$ . [see kernels](#)

We find eigendensities  $\psi$  and eigenvalues  $\sigma \in \mathbb{R}$ .

# Specialized quadratures (Martensen, 1963), (Kussmaul, 1969)

We rewrite the kernels  $L(t, \tau)$ ,  $M(t, \tau)$  in the form:

$$f(t, \tau) = f_1(t, \tau) \ln \left( 4 \sin^2 \frac{t - \tau}{2} \right) + f_2(t, \tau),$$

where  $f_1, f_2$  are smooth.

# Specialized quadratures (Martensen, 1963), (Kussmaul, 1969)

We rewrite the kernels  $L(t, \tau), M(t, \tau)$  in the form:

$$f(t, \tau) = f_1(t, \tau) \ln \left( 4 \sin^2 \frac{t - \tau}{2} \right) + f_2(t, \tau),$$

where  $f_1, f_2$  are smooth.

Integral		Quadrature
$\int_0^{2\pi} f_1(t, \tau) \ln \left( 4 \sin^2 \frac{t - \tau}{2} \right) d\tau$		Martensen and Kussmaul (p. 78 (Colton et al., 2013))
$\int_0^{2\pi} f_2(t, \tau) d\tau$		Trapezoidal rule.

Table 3: Use of quadratures. [see quads](#)

# Specialized quadratures (Martensen, 1963), (Kussmaul, 1969)

We rewrite the kernels  $L(t, \tau), M(t, \tau)$  in the form:

$$f(t, \tau) = f_1(t, \tau) \ln \left( 4 \sin^2 \frac{t - \tau}{2} \right) + f_2(t, \tau),$$

where  $f_1, f_2$  are smooth.

Integral		Quadrature
$\int_0^{2\pi} f_1(t, \tau) \ln \left( 4 \sin^2 \frac{t - \tau}{2} \right) d\tau$		Martensen and Kussmaul (p. 78 (Colton et al., 2013))
$\int_0^{2\pi} f_2(t, \tau) d\tau$		Trapezoidal rule.

Table 3: Use of quadratures. [see quads](#)

To observe exponential convergence, we replace  $f_1, f_2$  by their trigonometric interpolating polynomials (sec. 3.5 in (Colton et al., 1983), sec. 12.4 in (Kress, 1999)).

# Generalized eigenvalue problem I

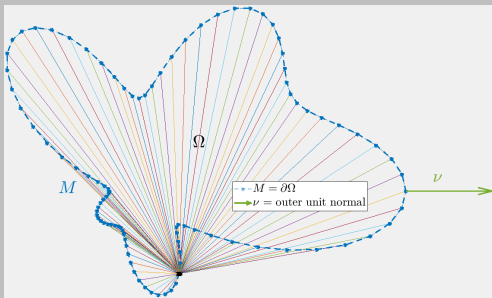


Figure 2: Discretized boundary  $M$  into  $2N$  equidistant points. Black dot is fixed point  $x_i \in M$ .

$$\text{We get a generalized EVP of size } 2N, \underbrace{(A_\mu + Id)}_{K'_\mu + I} \psi = \sigma \underbrace{B_\mu}_{\tilde{S}_\mu} \psi. \quad (1)$$

We solve for **eigendensity**  $\psi$  and **eigenvalues**  $\sigma$  using MATLAB's function `eig` / `eigs`.

## GEVP matrix structure

$$A_\mu = \begin{bmatrix} A_{0,0} & A_{0,1} & \cdots & A_{0,2N-1} \\ \vdots & \vdots & \ddots & \vdots \\ A_{2N-1,0} & A_{2N-1,1} & \cdots & A_{2N-1,2N-1} \end{bmatrix}, \text{ and similarly for } {}_{2N}[B_\mu]^{2N}.$$

For  $k, j : 0 \rightarrow 2N - 1$ ,

$$A_{k,j} = R^N(t_k, t_j)L_1(t_k, \tau_j) + \frac{\pi}{N}L_2(t_k, \tau_j),$$

$$B_{k,j} = R^N(t_k, \tau_j)M_1(t_k, \tau_j) + \frac{\pi}{N}M_2(t_k, \tau_j),$$

$$\sigma = \text{diag}(\sigma_0, \dots, \sigma_{2N-1}).$$

Here  $R^N$  are the weights of the Kress quadrature, and  $L_i, M_i, i = 1, 2$  are the kernels  $L, M$  re-written in the form  $f(t, \tau) = f_1(t, \tau) \ln\left(4 \sin^2 \frac{t-\tau}{2}\right) + f_2(t, \tau)$ .

## Generalized eigenvalue problem II

- Recall: if  $\mu \rightarrow \mu_D^-$  (mult.  $\ell$ ), then  $B\mu_D \rightarrow$  singular.
- Consider truncated SVD  $B\mu_D = \hat{U}\hat{\Sigma}\hat{V}^*$ ,  $\hat{\Sigma}$  has size  $r = 2N - \ell$ .

## Generalized eigenvalue problem II

- Recall: if  $\mu \rightarrow \mu_D^-$  (mult.  $\ell$ ), then  $B\mu_D \rightarrow$  singular.
- Consider truncated SVD  $B\mu_D = \hat{U}\hat{\Sigma}\hat{V}^*$ ,  $\hat{\Sigma}$  has size  $r = 2N - \ell$ .

We therefore solve for **eigendensity**  $\hat{\psi}$  and **eigenvalues**  $\hat{\sigma}$  using MATLAB's function `eig` / `eigs`,

$$\hat{U}^* \underbrace{(A_{\mu_D} + Id)}_{K'_{\mu_D} + I} \hat{V} \hat{\psi} = \hat{\sigma} \hat{U}^* \underbrace{B_{\mu_D}}_{S_{\mu_D}} \hat{V} \hat{\psi}. \quad (2)$$

The eigendensities of the original problem are  $\psi = \hat{V} \hat{\psi}$ .

# Algorithm

Recall the standard and SVD EVPs,

$$\underbrace{(A_{\mu} + Id)}_{K'_{\mu} + I} \psi = \sigma \underbrace{B_{\mu}}_{\tilde{S}_{\mu}} \psi, \quad (1)$$

$$\hat{U}^* \underbrace{(A_{\mu_D} + Id)}_{K'_{\mu_D} + I} \hat{V} \hat{\psi} = \hat{\sigma} \hat{U}^* \underbrace{B_{\mu_D}}_{S_{\mu_D}} \hat{V} \hat{\psi}. \quad (2)$$

# Algorithm

Recall the standard and SVD EVPs,

$$\underbrace{(A_{\mu} + Id)}_{K'_{\mu} + I} \psi = \sigma \underbrace{B_{\mu}}_{\tilde{S}_{\mu}} \psi, \quad (1)$$

$$\hat{U}^* \underbrace{(A_{\mu_D} + Id)}_{K'_{\mu_D} + I} \hat{V} \hat{\psi} = \hat{\sigma} \hat{U}^* \underbrace{B_{\mu_D}}_{S_{\mu_D}} \hat{V} \hat{\psi}. \quad (2)$$

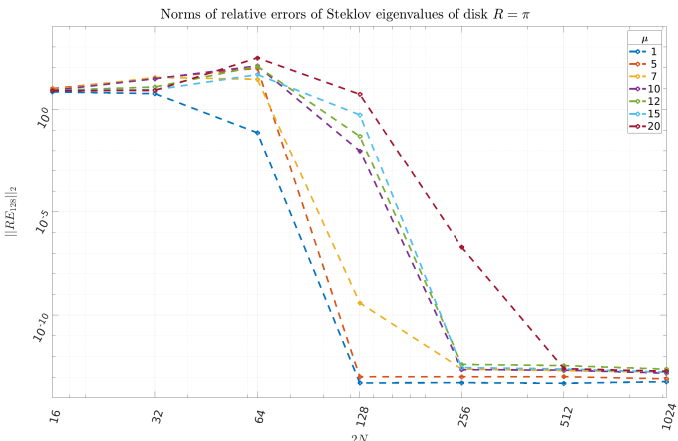
- **Inputs:** Curve details,  $N_1 \ll N$ ,  $\mu$  and tolerance.
- For a coarse grid with  $2N_1$  points, compute SVD of  $B_{\mu}$ .
- Is any singular value of  $B_{\mu}$  below tolerance ?
  - **Yes:** compute spectrum with SVD approach (2) and  $N$ .
  - **No:** compute spectrum using (1) and  $N$ .

## Steklov-Helmholtz EVP on a disk

[see others](#)

On a disk of radius  $R$ , the Steklov-Helmholtz eigenfunction is  $u_k(r, \theta) = J_k(\mu r)e^{ik\theta}$ .

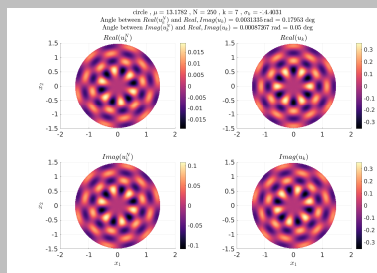
The corresponding eigenvalue is  $\sigma_k^{\text{true}} = \frac{\mu J'_k(\mu R)}{J_k(\mu R)}$ .  $\|RE_m\|_2 := \sqrt{\sum_{k=1}^m \frac{|\sigma_k^{\text{true}} - \sigma_k|^2}{|\sigma_k^{\text{true}}|^2}}$ .



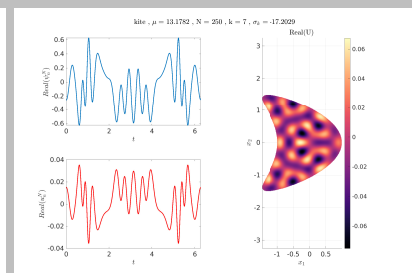
# Constructing the eigenfunctions inside $\Omega$

We use the **eigendensity**  $\psi$  to construct **eigenfunctions**  $\psi$  with the single layer and the trapezoidal rule,

$$u_k(x_j) = \int_0^{2\pi} \frac{i}{4} H_0^1(\mu r(x_j, \tau)) \psi_k(\tau) |x'(\tau)| d\tau.$$



(a) An eigenfunction for a disk



(b) An eigenfunction for the kite

# Steklov-Helmholtz EVP on domains of genus 1

Now  $M = \cup_{i=1}^2 M_i$ . The problem becomes: for fixed  $\mu$  find  $u, \sigma$  so that,

$$\begin{cases} -\Delta u - \mu^2 u = 0 & \text{in } \Omega, \\ \frac{\partial u}{\partial \nu_2} = \sigma \rho u & \text{on } M_2, \\ \frac{\partial u}{\partial \nu_1} = \sigma \rho u & \text{on } M_1. \end{cases}$$

For  $i = 1, 2$  with  $x_i \in M_i$  and denoting  $\nu_{x_i} := \nu_i$  the Steklov boundary condition gives, [see system](#)

$$\sum_{j=1}^2 \int_{M_j} \partial_{\nu_{x_i}} G_\mu(x_i, y) \psi_j(y) ds_y + \frac{\psi_i(x_i)}{2}$$

$$= \sigma \sum_{j=1}^2 \int_{M_j} G_\mu(x_i, y) \psi_j(y) ds_y.$$

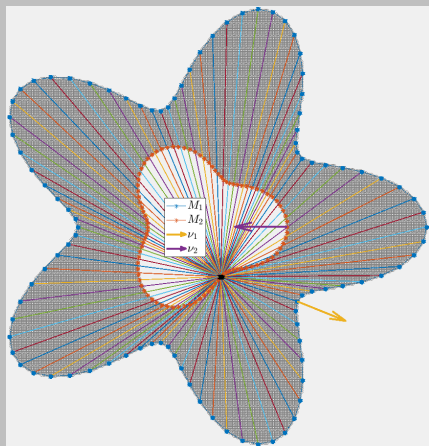


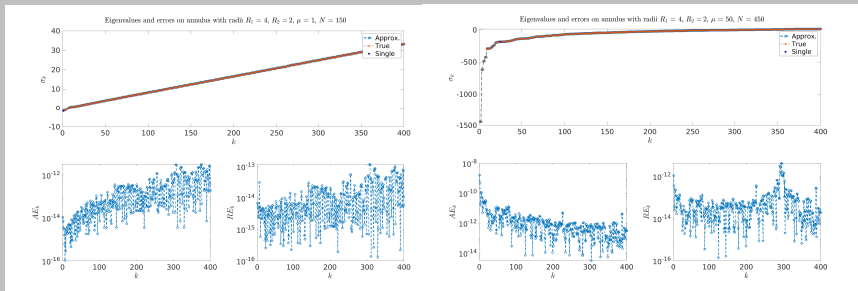
Figure 4:  $M$  is smooth enough, block dot is fixed  $x_{k,2}$  on  $M_2$ .

## Convergence of Steklov-Helmholtz eigenvalues on an annulus

[see true solution](#)

$$AE_k := |\sigma_k^{true} - \sigma_k|,$$

$$RE_k := |\sigma_k^{true} - \sigma_k| / |\sigma_k^{true}|.$$



(a) For  $N = 150, \mu = 1$ , we are able to recover the first 400 eigenvalues

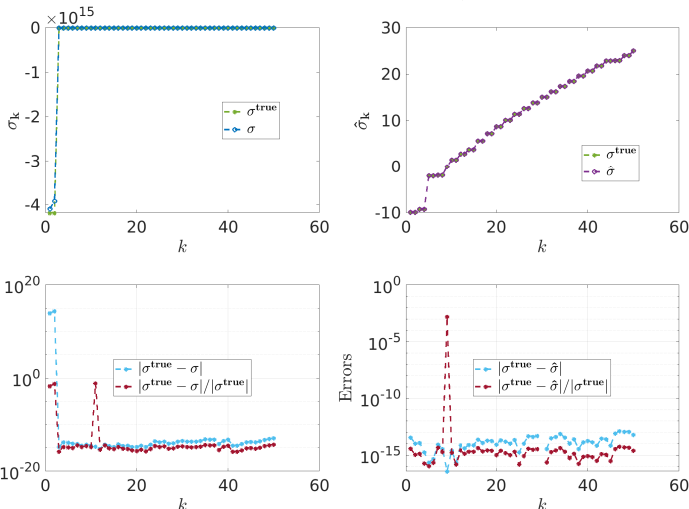
(b) For  $N = 450, \mu = 50$ , we are able to recover the first 400 eigenvalues .

Figure 5: Errors of the Steklov-Helmholtz eigenvalues for annulus of radii  $R_1 = 2$  and  $R_2 = 4$ .

[see turning](#)

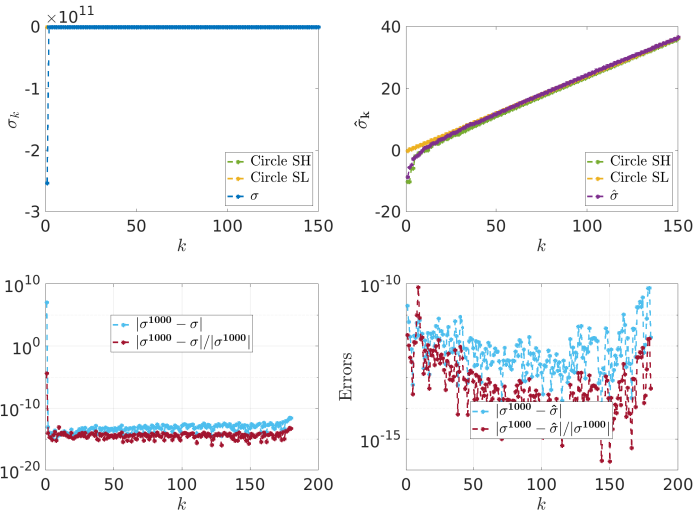
# Non SVD and SVD approach I

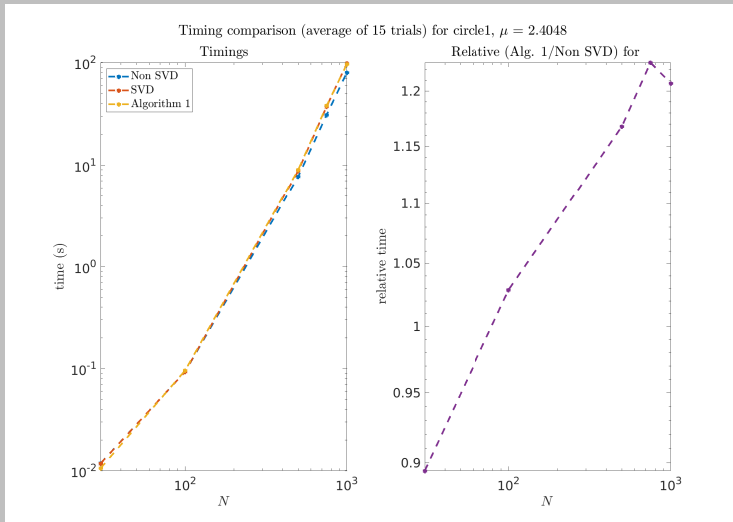
Errors of eigenvalues computed as is and via reduced SVD of SLP for circle1,  $\mu_{D,N} \approx 10.1735$ , N = 50, tol = -3,  $\Omega$  scale = 1



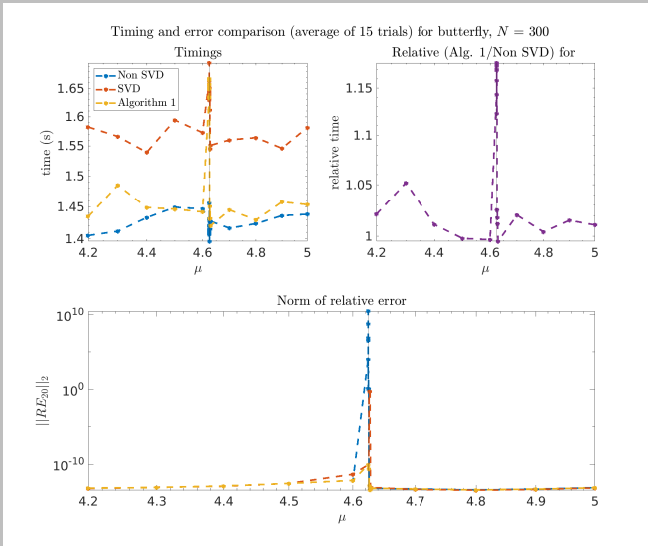
# Non SVD and SVD approach II

Errors of eigenvalues computed as is and via reduced SVD of SLP for butterfly,  $\mu_D \approx 4.6241$ ,  $N = 300$ , tol = -3,  $\Omega$  scale = 1



Timing: at  $\mu_D$ 

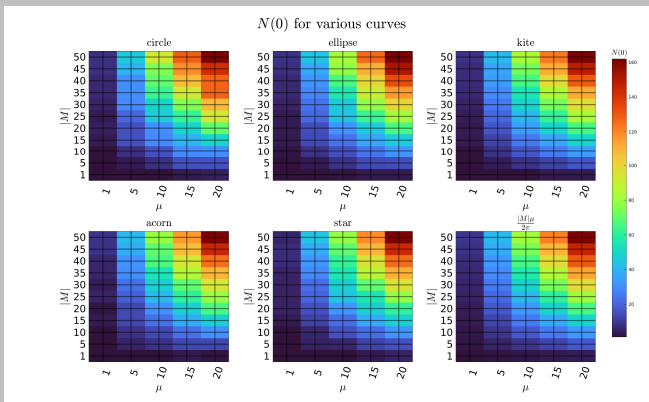
# Timing and errors: around $\mu_D$ , $N = 300$



# Negative eigenvalues of the Steklov-Helmholtz EVP

Consider the counting function of the eigenvalues,

$$N(x) := N_{SH}(x) = \#\{k \in \mathbb{N}, \sigma_k \leq x\}, \text{ we observe } N(0) \approx \frac{|M|\mu}{2\pi}.$$



# Asymptotics I

We attempt to **fit** to Steklov-Helmholtz eigenvalues functions of type,

$$\sigma_k(\Omega, \mu) \approx A_{\mu,|M|} k + B_{\mu,|M|} \sqrt{k} + \frac{C_{\mu,|M|}}{\sqrt{k}} + D_{\mu,|M|}.$$

[see fits](#)

# Asymptotics I

We attempt to **fit** to Steklov-Helmholtz eigenvalues functions of type, [see fits](#)

$$\sigma_k(\Omega, \mu) \approx A_{\mu,|M|} k + B_{\mu,|M|} \sqrt{k} + \frac{C_{\mu,|M|}}{\sqrt{k}} + D_{\mu,|M|}.$$

We observe that as  $k \rightarrow \infty$ , [see comparison](#)

$$\sigma_k(\Omega) \approx \frac{k\pi}{|M|} + \mathcal{O}(1), \text{ similar to the Steklov-Laplace EVP.}$$

# Asymptotics I

We attempt to **fit** to Steklov-Helmholtz eigenvalues functions of type, [see fits](#)

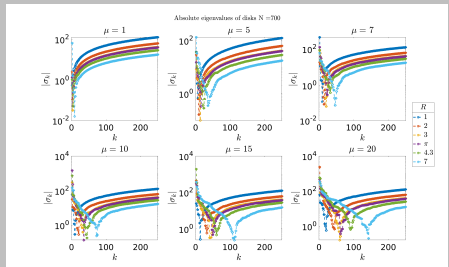
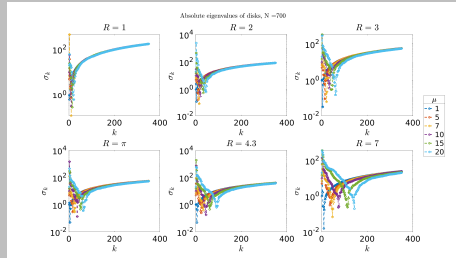
$$\sigma_k(\Omega, \mu) \approx A_{\mu, |M|} k + B_{\mu, |M|} \sqrt{k} + \frac{C_{\mu, |M|}}{\sqrt{k}} + D_{\mu, |M|}.$$

We observe that as  $k \rightarrow \infty$ , [see comparison](#)

$$\sigma_k(\Omega) \approx \frac{k\pi}{|M|} + \mathcal{O}(1), \text{ similar to the Steklov-Laplace EVP.}$$

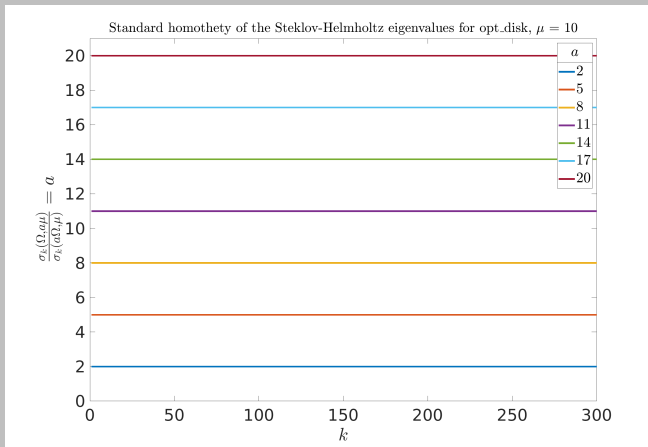
We also observe that the *early* part of the spectrum holds information about  $\mu, |M|, \kappa$ .

# Asymptotics II: Can we tell apart $|M|, \mu$ ?



# Homothety

$$\sigma_k(a\Omega, 0) = \frac{\sigma_k(\Omega, 0)}{a}, \quad \sigma_k(a\Omega, \mu) = \frac{\sigma_k(\Omega, a\mu)}{a}.$$



## Ongoing work

- Proving error estimates for the numerical method.

## Ongoing work

- Proving error estimates for the numerical method.
- Experiments on shape optimization for  $\sigma_k$ .

## Ongoing work

- Proving error estimates for the numerical method.
- Experiments on shape optimization for  $\sigma_k$ .
- Inclusion of  $\mu \in \mathbb{C}$ .

### Ongoing work

- Proving error estimates for the numerical method.
- Experiments on shape optimization for  $\sigma_k$ .
- Inclusion of  $\mu \in \mathbb{C}$ .

### Future work

- Allowing curves to be piecewise smooth with corners.

Ongoing work

- Proving error estimates for the numerical method.
- Experiments on shape optimization for  $\sigma_k$ .
- Inclusion of  $\mu \in \mathbb{C}$ .

Future work

- Allowing curves to be piecewise smooth with corners.
- Extending this work to  $\mathbb{R}^3$ .

-  Steklov, Vladimir (1895). *AimPL: Steklov eigenproblems*. American institute of Mathematics. URL: <http://aimpl.org/stekloveigen>.
-  WEINSTOCK, ROBERT (1954). "Inequalities for a Classical Eigenvalue Problem". In: *Journal of Rational Mechanics and Analysis* 3, pp. 745–753. ISSN: 19435282, 19435290. URL: <http://www.jstor.org/stable/24900312> (visited on 08/16/2023).
-  Martensen, Erich (1963). "Über eine Methode zum räumlichen Neumannschen Problem mit einer Anwendung für torusartige Berandungen". In: *Acta Mathematica* 109.none, pp. 75–135. DOI: [10.1007/BF02391810](https://doi.org/10.1007/BF02391810). URL: <https://doi.org/10.1007/BF02391810>.
-  Kussmaul, R. (1969). "Ein numerisches Verfahren zur Lösung des Neumannschen Außenraumproblems für die Helmholtzsche Schwingungsgleichung". In: *Computing* 4. URL: <https://doi.org/10.1007/BF02234773>.
-  Hersch, Joseph E., Lawrence Edward Payne, and Menahem M. Schiffer (1974). "Some inequalities for Stekloff eigenvalues". In: *Archive for Rational Mechanics and Analysis* 57, pp. 99–114.

-  Colton, David and Rainer Kress (1983). *Integral Equation Methods in Scattering Theory*. Society for Industrial and Applied Mathematics. URL: <https://pubs.siam.org/doi/abs/10.1137/1.9781611973167>.
-  Tang, Wei-jun, Zhi Guan, and Hou-de Han (1998). "Boundary element approximation of Steklov eigenvalue problem for Helmholtz equation". In: *Journal of Computational Mathematics*, pp. 165–178.
-  Kress, Rainer (1999). *Linear integral equations*.
-  McLean, William C. (2000). *Strongly Elliptic Systems and Boundary Integral Equations*. Cambridge University Press. ISBN: 9780521663755.
-  Carr, J. et al. (Sept. 2001). "Reconstruction and Representation of 3D Objects With Radial Basis Functions". In: *ACM SIGGRAPH*. DOI: [10.1145/383259.383266](https://doi.org/10.1145/383259.383266).
-  Huang, Jin and Tao Lü (2004). "THE MECHANICAL QUADRATURE METHODS AND THEIR EXTRAPOLATION FOR SOLVING BIE OF STEKLOV EIGENVALUE PROBLEMS". In: *Journal of Computational Mathematics* 22.5, pp. 719–726. ISSN: 02549409, 19917139. URL: <http://www.jstor.org/stable/43693198> (visited on 09/09/2023).

-  Betcke, Timo and Lloyd N. Trefethen (2005). "Reviving the Method of Particular Solutions". In: *SIAM Rev.* 47, pp. 469–491.
-  Fraser, Ailana and Richard Schoen (Dec. 2009). "The first Steklov eigenvalue, conformal geometry, and minimal surfaces". In.
-  Girouard, Alexandre and Iosif Polterovich (June 2010). "On the Hersch-Payne-Schiffer inequalities for Steklov eigenvalues". In: *Functional Analysis and Its Applications* 44, pp. 106–117. DOI: [10.1007/s10688-010-0014-1](https://doi.org/10.1007/s10688-010-0014-1).
-  Delfour, M. C. and J. -P. Zolésio (2011). *Shapes and Geometries*. Second. Society for Industrial and Applied Mathematics. DOI: [10.1137/1.9780898719826](https://doi.org/10.1137/1.9780898719826). eprint: <https://pubs.siam.org/doi/pdf/10.1137/1.9780898719826>. URL: <https://pubs.siam.org/doi/abs/10.1137/1.9780898719826>.
-  Arendt, Wolfgang and Rafe Mazzeo (Nov. 2012). "Friedlander's eigenvalue inequalities and the Dirichlet-to-Neumann semigroup". In: *Communications on Pure and Applied Analysis* 11. DOI: [10.3934/cpaa.2012.11.2201](https://doi.org/10.3934/cpaa.2012.11.2201).
-  Fraser, Ailana and Richard Schoen (Sept. 2012). "Eigenvalue bounds and minimal surfaces in the ball". In: *Inventiones mathematicae* 203.

-  Colton, David and Rainer Kress (2013). *Inverse acoustic and electromagnetic scattering theory, third edition*. ISBN: 9781461449423 1461449421. URL: <http://link.springer.com/book/10.1007%2F978-1-4614-4942-3>.
-  Akhmetgaliyev, Eldar, Oscar Bruno, and Nilima Nigam (Nov. 2014). "A boundary integral algorithm for the Laplace Dirichlet-Neumann mixed eigenvalue problem". In: *Journal of Computational Physics* 298. DOI: [10.1016/j.jcp.2015.05.016](https://doi.org/10.1016/j.jcp.2015.05.016).
-  Kuznetsov, Nikolay G. et al. (2014). "The legacy of Vladimir Andreevich Steklov". In: *Notices of the American Mathematical Society* 61, pp. 9–23.
-  Cakoni, Fioralba, David Colton, et al. (Jan. 2016). "Stekloff Eigenvalues in Inverse Scattering". In: *SIAM Journal on Applied Mathematics* 76, pp. 1737–1763. DOI: [10.1137/16M1058704](https://doi.org/10.1137/16M1058704).
-  Akhmetgaliyev, Eldar, Chiu-Yen Kao, and Braxton Osting (2017). "Computational methods for extremal Steklov problems". In: *SIAM Journal on Control and Optimization* 55.2, pp. 1226–1240.
-  Bucur, Dorin, Pedro Freitas, and James Kennedy (Jan. 2017). *4 The Robin problem*. ISBN: 9783110550887. DOI: [10.1515/9783110550887-004](https://doi.org/10.1515/9783110550887-004).

-  Cakoni, Fioralba and Rainer Kress (2017). "A boundary integral equation method for the transmission eigenvalue problem". In: *Applicable Analysis* 31.2, pp. 23–38. DOI: [10.1080/00036811.2016.1189537](https://doi.org/10.1080/00036811.2016.1189537).
-  Girouard, Alexandre and Iosif Polterovich (2017). "Spectral geometry of the Steklov problem (survey article)". In: *Journal of Spectral Theory* 7.2, pp. 321–359.
-  Wang, Yu et al. (2018). "Steklov Spectral Geometry for Extrinsic Shape Analysis". In: *ACM Transactions on Graphics* 38. DOI: <https://doi.org/10.1145/3152156>.
-  Alhejaili, Weaam and Chiu-Yen Kao (2019). "Numerical studies of the Steklov eigenvalue problem via conformal mappings". In: *Applied Mathematics and Computation* 347, pp. 785–802.
-  Meng, Jian and Liquan Mei (2020). "Discontinuous Galerkin methods of the non-selfadjoint Steklov eigenvalue problem in inverse scattering". In: *Applied Mathematics and Computation* 381, p. 125307.

-  Antunes, Pedro R.S. (2021). "Numerical calculation of extremal Steklov eigenvalues in 3D and 4D". In: *Computers and Mathematics with Applications* 104, pp. 50–58. ISSN: 0898-1221. DOI: <https://doi.org/10.1016/j.camwa.2021.11.008>. URL: <https://www.sciencedirect.com/science/article/pii/S0898122121004053>.
-  Girouard, Alexandre, Mikhail Karpukhin, et al. (Feb. 2021). "The Dirichlet-to-Neumann map, the boundary Laplacian, and Hörmander's rediscovered manuscript". In.
-  Oudet, Edouard, C.-Y Kao, and Braxton Osting (Mar. 2021). "Computation of free boundary minimal surfaces via extremal Steklov eigenvalue problems". In: *ESAIM: Control, Optimisation and Calculus of Variations* 27. DOI: <10.1051/cocv/2021033>.
-  Turk, Onder (Jan. 2021). "A DRBEM approximation of the Steklov eigenvalue problem". In: *Engineering Analysis with Boundary Elements* 122, pp. 232–241. DOI: <10.1016/j.enganabound.2020.11.003>.
-  Caubet, Fabien, Marc Dambrine, and Rajesh Mahadevan (Aug. 2022). "Shape Sensitivity of Eigenvalue Functionals for Scalar Problems: Computing the Semi-derivative of a Minimum". In: *Applied Mathematics & Optimization* 86. DOI: <10.1007/s00245-022-09827-6>.

-  Imeri, Kthim and Nilima Nigam (2022). *A Steklov-spectral approach for solutions of Dirichlet and Robin boundary value problems.* arXiv: 2209 . 08405 [math.NA].
-  Levitin, Michael, Dan Mangoubi, and Iosif Polterovich (2022). *Topics in spectral geometry.* Cambridge University Press.
-  Ma, Y. and J. Sun (2022). "Integral Equation Method for a Non-Selfadjoint Steklov Eigenvalue Problem.". In: *Communications in Computational Physics*. DOI: 10.4208/cicp.0A-2022-0016.
-  Chaigneau, Adrien and Denis S. Grebenkov (Sept. 2023). "A numerical study of the Dirichlet-to-Neumann operator in planar domains". In: arXiv: 2310.19571 [cs.NA].

## Brief literature survey: Steklov EVP

[see summary L](#)[see summary H](#)

(Girouard and Polterovich, 2017) extensively review the Laplace Steklov EVP. Chapter 7 in (Levitin et al., 2022) is on the Steklov EVP.

### Optimization for Steklov-Laplace EVP:

- (Akhmetgaliyev, Kao, et al., 2017) use layer potentials and gradient based optimization for  $|M|\sigma_k$ . Extended to 3D and 4D in (Antunes, 2021).
- (Alhejaili et al., 2019) use Fourier series expansions, conformal maps and gradient based optimization for  $\sqrt{|\Omega|}\sigma_k$ .

### Modified Steklov-Helmholtz EVP: The modified Helmholtz operator is $-\Delta + \mu^2$ .

- In (Tang et al., 1998) the Steklov EVP with  $\mu = 1$  is solved by using layer potentials. Report relative errors of low order for the disk.
- (Chaigneau et al., 2023) focus on the relation between the spectrum and the geometric structure of the domain using finite elements.

### Steklov-Helmholtz EVP: $\mu \in \mathbb{C}$

- In (Meng et al., 2020), 3 different DG discretization schemes are compared.
- In (Ma et al., 2022), layer potentials with the spectral indicator method are used to locate  $\sigma$ .

## Applications (Cakoni, Colton, et al., 2016) (Chaigneau et al., 2023)

[back to intro.](#)

In inverse scattering, changes in the refractive index of an inhomogeneous medium of compact support can be determined from changes in measured far field data due to incident plane waves using the Steklov boundary condition.

In electrical impedance tomography, the conductivity inside is to be determined from measurements on the boundary. Allows for instance lung function assessment.

Geophysics for imaging sub-surface structures.

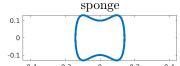
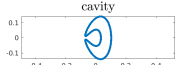
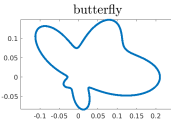
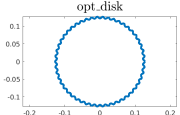
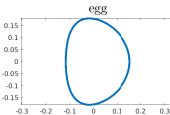
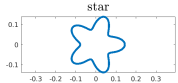
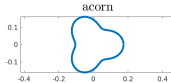
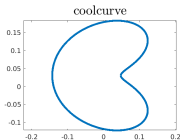
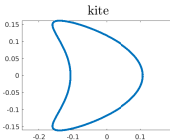
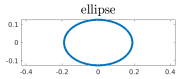
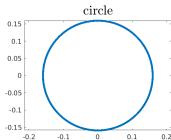
Recent theoretical description of diffusion-controlled reactions relies on the eigenbasis of the DtN operator to decompose the propagators.

In transmission eigenvalues.

# Curves

[back to contrib.](#)

$$|M| = 1$$



# Properties of $-\Delta - \mu^2$

[back to Helmholtz](#)

$$L = \sum_{i,j=1}^2 a^{ij} \partial_{x_i x_j} + c = -\Delta - \mu^2 \implies A = [a^{ij}] = Id, \quad c = -\mu^2$$

$L$  is uniformly elliptic if there is a constant  $\theta > 0$  such that

$$\sum_{i,j=1}^2 a^{ij} \xi_i \xi_j \geq \theta |\xi|^2 \text{ for all } \xi \in \mathbb{R}^2$$

We have  $\sum_{i,j=1}^2 a^{ij} \xi_i \xi_j = \xi_1^2 + \xi_2^2 = |\xi|^2 \implies \theta = 1$ . Associated bilinear form is

$$\Phi(u, v)_\Omega = \int_\Omega \nabla \bar{u} \cdot \nabla v - \mu^2 \bar{u} v = \overline{\int_\Omega \nabla u \cdot \nabla \bar{v} - \mu^2 u \bar{v}}.$$

For real wave number  $\mu$ ,

$$\Phi(u, v)_\Omega = \overline{\Phi(v, u)_\Omega},$$

## Why not Dirichlet-Laplace EV

[back to SH EVP.](#)

Suppose  $U$  solves the Dirichlet problem and  $U^D$  is an eigen function of the homogeneous Dirichlet problem. Then consider in  $\Omega$  for  $\alpha \in \mathbb{R}$ ,

$$-\Delta(U + \alpha U^D) = -\Delta U - \alpha \Delta U^D = \mu^2(U + \alpha U^D)$$

and on  $M$ ,  $TU + \alpha TU^D = TU = u$ .

# Maps

[back to LP](#)

Let  $\Omega$  be  $C^{r+1,1}$ ,  $r \geq 0$ . Then by theorems 3.37 and 4.21 in (McLean, 2000),

- $\mathcal{E}_\mu : H^{s+1/2}(M) \rightarrow H^{s+1}(\Omega)$ ,  $0 \leq s \leq r + 1$ .
- $T : H^{s+1}(\Omega) \rightarrow H^{s+1/2}(M)$ ,  $-1/2 < s \leq r + 1$ .
- The linear operator

$$\mathcal{D}_\mu : H^{s+1/2}(M) \rightarrow H^{s-1/2}(M), \quad \mathcal{D}_\mu : u \mapsto T\partial_\nu(\mathcal{E}_\mu u)$$

is called the **Dirichlet to Neumann (DtN)** map for the Helmholtz equation.

- $\mathcal{S}_\mu = \mathcal{E}_\mu \tilde{\mathcal{S}}_\mu$  and  $\tilde{\mathcal{S}}_\mu = T\mathcal{S}_\mu$ .
- $\mathcal{D}_\mu \phi = (K'_\mu + I)\tilde{\mathcal{S}}_\mu^{-1}\phi$  (Cor. 2.3 Cakoni and Kress, 2017).
- We work with  $s = 0$ .

# Sobolev spaces of periodic functions I

[back to LP](#)

Let  $f \in L^2[0, 2\pi]$ , with its Fourier series:

$$f(t) = \sum_{i \in \mathbb{Z}} a_i e^{i j t}, \quad a_j = \frac{1}{2\pi} \int_0^{2\pi} \frac{f(t)}{e^{i j t}} dt.$$

For  $f, g \in L^2[0, 2\pi]$  recall the standard inner-product and induced norm

$$(f, g) = \int_0^{2\pi} f \overline{g}, \quad \|f\|_2^2 = \int_0^{2\pi} |f|^2$$

The set  $\{e^{ijt}\}_{j \in \mathbb{Z}}$  is orthonormal and dense in  $C[0, 2\pi]$  with the sup-norm.

$C[0, 2\pi]$  is dense in  $L^2[0, 2\pi]$  with the  $\|\cdot\|_2$ -norm. So  $\{e^{ijt}\}$  is complete and the Fourier series of  $f$  converges in the  $\|\cdot\|_2$ -norm.

Parseval's equality then gives  $\|f\|_2^2 = 2\pi \sum_j |a_j|^2$ .

## Sobolev spaces of periodic functions II

[back to LP](#)

Recall  $f \in L^2[0, 2\pi]$ , with its Fourier series:

$$f(t) = \sum_{i \in \mathbb{Z}} a_j e^{ijt}, \quad a_j = \frac{1}{2\pi} \int_0^{2\pi} \frac{f(t)}{e^{ijt}} dt.$$

Let  $0 \leq p < \infty$ . The Sobolev space  $H^p[0, 2\pi]$  is defined as

$$H^p[0, 2\pi] = \{f \in L^2[0, 2\pi], \quad \|f\|_{H^p} < \infty\}, \text{ where } \|f\|_{H^p} = \left( \sum_{j \in \mathbb{Z}} (1 + j^2)^p |a_j|^2 \right)^{1/2}.$$

Let  $f, g \in H^p[0, 2\pi]$  with Fourier coefficients  $a_j, b_j$  respectively. Then  $H^p[0, 2\pi]$  is a Hilbert space with respect to the inner-product:

$$(f, g)_{H^p} = \sum_{j \in \mathbb{Z}} (1 + j^2)^p a_j \overline{b_j}.$$

## Kernels

[Back to reformulation](#)

$$r(t, \tau)^2 = (z_1(t) - z_1(\tau))^2 + (z_2(t) - z_2(\tau))^2$$

$$X(t, \tau) := [z'_2(t)(z_1(\tau) - z_1(t)) - z'_1(t)(z_2(\tau) - z_2(t))]$$

$$L(t, \tau) := \frac{i\mu}{2|z'(t)|} \frac{H_1^1(\mu r(t, \tau))}{r(t, \tau)} X(t, \tau) |z'(\tau)| \text{ and } M(t, \tau) := \frac{i}{2} H_0^1(\mu r(t, \tau)) |z'(\tau)|$$

# Quadratures

[back to SQ](#)

$$\tau_j = \frac{\pi j}{N}, \quad j : 0 \rightarrow 2N - 1.$$

$$\int_0^{2\pi} f_1(t, \tau) \ln \left( 4 \sin^2 \frac{t - \tau}{2} \right) d\tau \approx \sum_{j=0}^{2N-1} R^N(t, \tau_j) f_1(t, \tau_j), \text{ where}$$

$$R^N(t, \tau_j) := -\frac{2\pi}{N} \sum_{m=1}^{N-1} \frac{\cos m(t - \tau_j)}{m} - \pi \frac{\cos N(t - \tau_j)}{N^2}, \quad j : 0 \rightarrow 2N - 1.$$

$$\int_0^{2\pi} f_2(t, \tau) d\tau \approx \frac{\pi}{N} \left( \frac{f_2(t, 0) + f_2(t, 2\pi)}{2} + \sum_{j=1}^{2N-1} f_2(t, \tau_j) \right) = \frac{\pi}{N} \sum_{j=0}^{2N-1} f_2(t, \tau_j).$$

## Generalized eigenvalue problem

$$A_\mu = \begin{bmatrix} A_{0,0} & A_{0,1} & \cdots & A_{0,2N-1} \\ \vdots & \vdots & \ddots & \vdots \\ A_{2N-1,0} & A_{2N-1,1} & \cdots & A_{2N-1,2N-1} \end{bmatrix}, \text{ and similarly for } {}_{2N}[B_\mu]^{2N}.$$

For  $k, j : 0 \rightarrow 2N - 1$ ,

$$A_{k,j} = R^N(t_k, t_j)L_1(t_k, \tau_j) + \frac{\pi}{N}L_2(t_k, \tau_j),$$

$$B_{k,j} = R^N(t_k, \tau_j)M_1(t_k, \tau_j) + \frac{\pi}{N}M_2(t_k, \tau_j).$$

$$\sigma = \text{diag}(\sigma_0, \dots, \sigma_{2N-1})$$

[back to GEVP](#)

## Standard Laplace EVPs

The discretized layer potentials can be used to solve the Dirichlet/Neumann/Robin EVPs.

### **Algorithm 1** Search for Laplace eigenvalues $\lambda^D$ , $\lambda^N$ and $\lambda^R$

**Require:** Curve details,  $\sigma$ ,  $[\mu_{\min}, \mu_{\max}]$  and number of points  $n_\mu$ .

Create vector of  $n_\mu$  equispaced wave numbers in  $[\mu_{\min}, \mu_{\max}]$  and 3 vectors of length of  $n_\mu$ ,  $s_{\min}^i$ ,  $i = D, N, R$  to store minimum singular values for each problem.

**for**  $j = 1, \dots, n_\mu$  **do**

$\mu = \mu_j$

Compute SVDs of  $B_\mu$ ,  $A_\mu + Id$  and  $C_\mu = -\sigma B_\mu + (A_\mu + Id)$ .

Find smallest singular value of each and store in  $j$ th element of respective  $s_{\min}^i$ ,  $i = D, N, R$ .

**end for**

## Standard Laplace EVPs on a disk

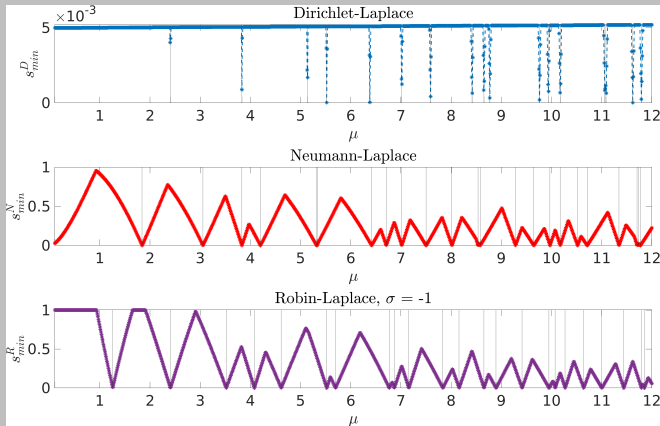


**Figure 7:** Minimum singular values of  $B_\mu$  (Dirichlet-Laplace,  $s_{min}^D$ , top, blue),  $A_\mu + Id$  (Neumann-Laplace,  $s_{min}^N$ , middle, red) and  $C_\mu$  (Robin-Laplace  $\sigma = -1$ ,  $s_{min}^R$ , bottom, purple) for the unit disk with  $\mu \in [0.1, 12]$ . Computed eigenvalues correspond to local minimas of  $s_{min}^i$ ,  $i = D, N, R$ . The vertical lines correspond to the true eigenvalues.

## Sign flipping and RBF interpolation

We convert the search problem to a root finding problem.

We first sign-flip (sec. 9 (Betcke et al., 2005)) the  $s_{min}$  curves near local minima and then interpolate using RBFs (Carr et al., 2001).

### Algorithm 2 RBF interpolation of function evaluations for $f$

**Require:** Evaluations  $\{f_i\}_{i=1}^m$ , evaluation points  $\{X_i = (x_i, y_i)\}_{i=1}^m$ , choice of rbf  $\phi$   
 The interpolation points are  $\text{rbf\_points} = \{X_i\}$  and the function to interpolate is  
 $\text{rbf\_f} = \{f_i\}$

Create meshgrid of  $x_i = [x_\tau, x_t]$  and  $y_i = [y_\tau, y_t]$

Compute the distance between all  $\text{rbf\_points}$  and store in  $\text{R\_rbf}$ .

Create matrix of rbf evaluations,  $\text{A\_rbf} = [\phi(x_t - x_\tau, y_t - y_\tau)]$

Compute the RBF coefficients  $\eta = \text{rbf\_coeffs} = \text{A\_rbf}^{-1} \text{rbf\_f}$

To compute the function value of the interpolant  $f_{RBF}$  at any point  $Z \subset \mathbb{R}^2$ , set

$f(Z) = 0$

**for**  $i = 1, \dots, m$  **do**

$$r_i = |Z - X_i|$$

$$f_{RBF}(Z) = f_{RBF}(Z) + \eta_i \phi(r_i)$$

**end for**

Use sign flipping as in (Betcke et al., 2005) on each  $s_{min}^i$  and then interpolate with inverse multiquadric RBF (Carr et al., 2001).

# A convergence study for the disk

[Back to SH disk](#)

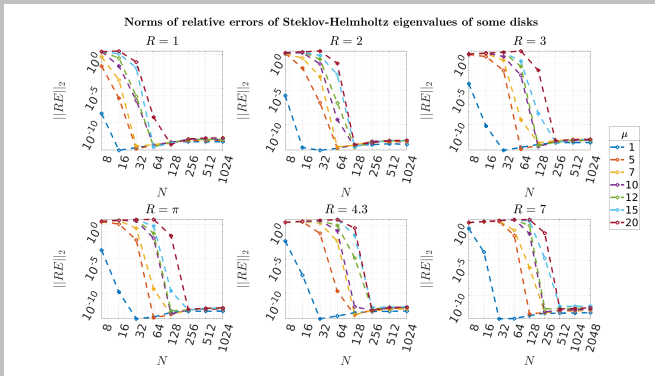


Figure 8: Norms of relative errors  $\|RE\|_2$  of  $\sigma_k$  against  $N$  across various disks and wave numbers  $\mu$  with respect to  $\sigma_k^{\text{true}}$ . In each subplot, we fix  $R$  and vary  $\mu$ .

## Convergence for some curves

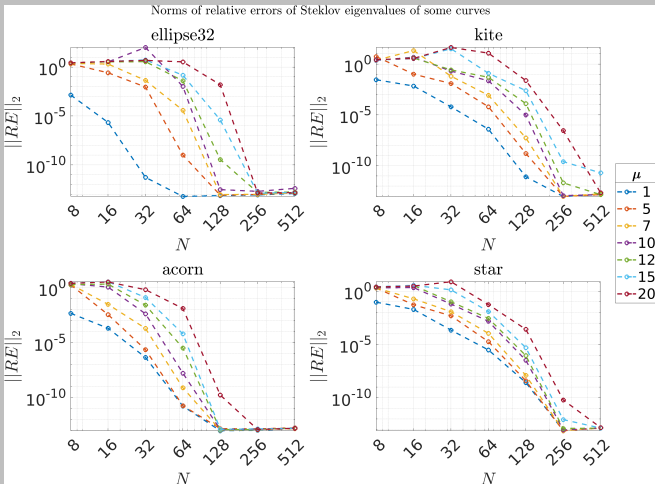
[Back to disk](#)

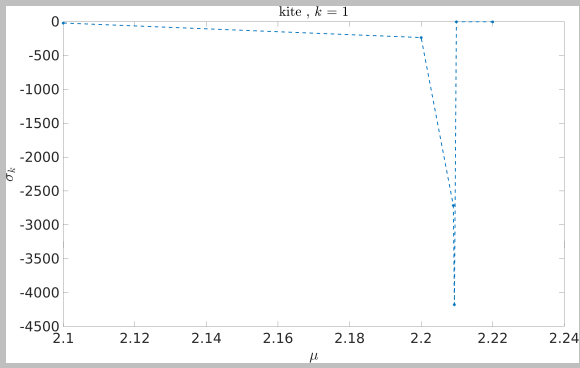
Figure 9: Convergence of Steklov-Helmholtz eigenvalues for some curves.

## Approaching Dirichlet-Laplace eigenvalues

For our method to work, we require that  $\mu^2$  is not a Dirichlet-Laplace eigenvalue. From theorem 7.4.8 in (Levitin et al., 2022) for  $\lambda^D$  of multiplicity  $m$ , as  $\mu^2 \rightarrow \lambda^D$  from the left,  $\sigma_i \rightarrow -\infty$ ,  $i = 1 \rightarrow m$ . We consider a kite such that for  $\mu_D \approx 2.20986$ ,  $\mu_D^2$  is a Dirichlet-Laplace eigenvalue.

$\sigma_1(\mu)$

State DL and SH problems side by side, and then explain.



# Ring system

[back to annulus setup](#)

Discretizing exactly like before, we have another set of  $4N$  equations and the following generalized eigenvalue problem:

$$\begin{pmatrix} A_1 + Id & \tilde{A}_2 \\ -\tilde{A}_1 & -A_2 + Id \end{pmatrix} \begin{pmatrix} \psi_1 \\ \psi_2 \end{pmatrix} = \tilde{\sigma} \begin{pmatrix} B_1 & \tilde{B}_2 \\ \tilde{B}_1 & B_2 \end{pmatrix} \begin{pmatrix} \psi_1 \\ \psi_2 \end{pmatrix}.$$

The  $2N \times 2N$  matrix  $A_1 + Id$  ( $B_1$ ) in equation (52) corresponds to the discretized adjoint of the double layer potential (single layer potential) which relates fixed points  $x_1 \in M_1$  to every point on  $M_1$ . The  $2N \times 2N$  matrix  $\tilde{A}_2$  ( $\tilde{B}_2$ ) in equation (52) corresponds to the discretized adjoint of the double layer potential (single layer potential) which relates fixed points  $x_1 \in M_1$  to every point on  $M_2$ . The  $2N \times 2N$  matrix  $-\tilde{A}_1$  ( $\tilde{B}_1$ ) in equation (52) corresponds to the discretized adjoint of the double layer potential (single layer potential) which relates fixed points  $x_2 \in M_2$  to every point on  $M_1$ . The  $2N \times 2N$  matrix  $-A_2 + Id$  ( $B_2$ ) in equation (52) corresponds to the discretized adjoint of the double layer potential (single layer potential) which relates fixed points  $x_2 \in M_2$  to every point on  $M_2$ .

## SH EVP solution on an annulus

[back to annulus error](#)

Consider a concentric annulus with inner and outer radii  $0 < R_2 \leq R_1$ . Compared to a single disk, the radial part of the solution of the Helmholtz equation is modified to  $AJ_n(\mu r) + BY_n(\mu r)$ . We get the system,

$$\begin{pmatrix} \tilde{\sigma}_n J_n(\mu R_1) - \mu J'_n(\mu R_1) & \tilde{\sigma}_n Y_n(\mu R_1) - \mu Y'_n(\mu R_1) \\ \tilde{\sigma}_n J_n(\mu R_2) + \mu J'_n(\mu R_2) & \tilde{\sigma}_n Y_n(\mu R_2) + \mu Y'_n(\mu R_2) \end{pmatrix} \begin{pmatrix} A \\ B \end{pmatrix} = \begin{pmatrix} 0 \\ 0 \end{pmatrix}.$$

We set the determinant to zero solution and obtain a quadratic equation in  $\tilde{\sigma}_n$ ,

$$\begin{pmatrix} J_n(\mu R_1)Y_n(\mu R_2) - J_n(\mu R_2)Y_n(\mu R_1) \\ \mu \left[ J_n(\mu R_1)Y'_n(\mu R_2) - J'_n(\mu R_1)Y_n(\mu R_2) - J'_n(\mu R_2)Y_n(\mu R_1) + J_n(\mu R_2)Y'_n(\mu R_1) \right] \\ \mu^2 \left[ -J'_n(\mu R_1)Y'_n(\mu R_2) + J'_n(\mu R_2)Y'_n(\mu R_1) \right] \end{pmatrix}^\top \begin{pmatrix} \tilde{\sigma}_n^2 \\ \tilde{\sigma}_n \\ 1 \end{pmatrix} = 0.$$

# Ring turning

[back to annulus error](#)

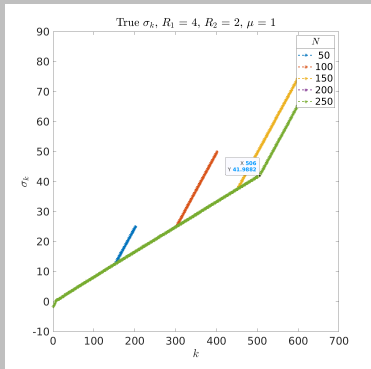


**Figure 11:** The true solution seems to turn at different points, till a certain value of  $N$ .

In this configuration, we can see that for  $150 \leq N \leq 200$ , the turning point does not move and is fixed near  $k = 506$ , which corresponds to a Bessel order of  $n = 168$ . Bessel functions of order more than 168 are either  $\pm \text{Inf}$  or  $\text{NaN}$  in MATLAB. For the same configuration, since the turning of the true eigenvalues occurs at different values of  $k$  on increasing  $N$ , we conclude that it is a false artifact arising possibly due to numerical errors for higher values of  $k$ .

# Homothetic property for Steklov-Helmholtz EVP

[back to homothety](#)

## Lemma

Let  $\sigma_k(\Omega, \mu)$  be the Steklov-Helmholtz eigenvalues for  $\Omega \subset \mathbb{R}^d$  ( $\Omega$  closed and bounded) with wave number  $\mu$  and consider the scaled domain

$a\Omega = \{x \in \Omega : x/a \in \Omega, a > 0\}$ . Then Steklov-Helmholtz eigenvalues share the scaling property with the Robin eigenvalue problem (equation 4.9 in (Bucur et al., 2017)) and in particular we have

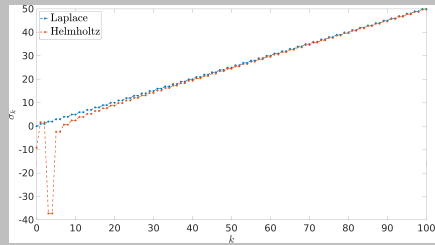
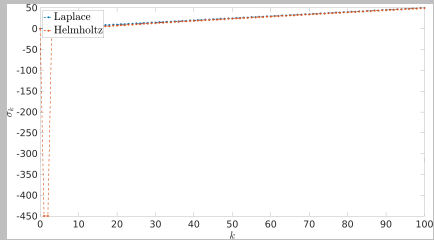
$$\sigma_k(a\Omega, \mu) = \frac{\sigma_k(\Omega, a\mu)}{a}.$$

The lemma follows by using the variational form of the Steklov-Helmholtz eigenvalues and a change of variables  $z = x/a$ .

If  $\mu = 0$ , we get back the Laplacian and its homothetic property for the Steklov-Laplace eigenvalues, i.e.

$$\sigma_k(a\Omega, 0) = \frac{\sigma_k(\Omega, 0)}{a}.$$

## Asymptotic comparison for the unit disk

[back to asymp.](#)(a)  $\mu = 5$ (b)  $\mu = 7$

# Asymptotic fits

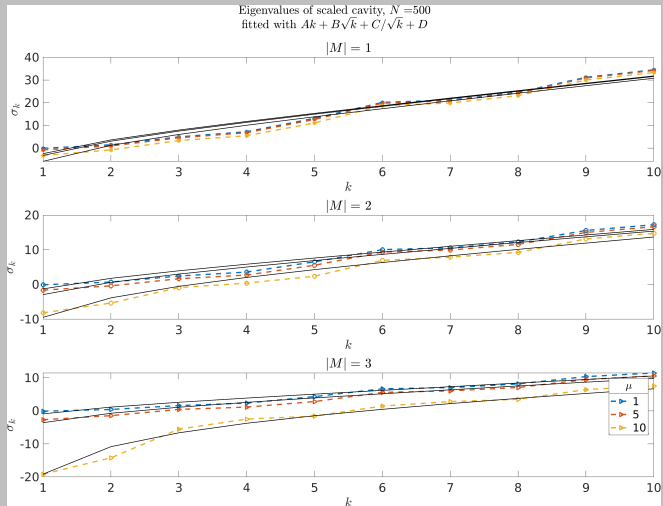
[back to asymp.](#)

Figure 13: Asymptotic fits for the cavity.

# Shape derivatives

[back to SO](#)

$$(|M|\sigma_k)' = |M| \int_M (|\nabla_\Gamma u|^2 - \mu^2|u|^2 - \sigma_k^2|u|^2 - \kappa\sigma_k|u|^2) v \cdot \nu ds + \sigma_k \int_M \kappa v \cdot \nu ds,$$

and

$$\left(\sqrt{|\Omega|}\sigma_k\right)' = \sqrt{|\Omega|} \int_M (|\nabla_\Gamma u|^2 - \mu^2|u|^2 - \sigma_k^2|u|^2 - \kappa\sigma_k|u|^2) v \cdot \nu ds + \frac{\sigma_k}{2\sqrt{|\Omega|}} \int_M v \cdot \nu ds,$$

where  $\kappa$  is the mean curvature of  $M$  and  $v$  is the velocity with respect to the parameters of the curve. Here, the tangential gradient is  $\nabla_\Gamma u = \nabla u - \partial_\nu u \nu$ .

# Shape optimization

We first note the homothety property of the Steklov-Helmholtz spectrum:

[see lemma](#)[see example](#)

$$\sigma_k(a\Omega, \mu) = \frac{\sigma_k(\Omega, a\mu)}{a}.$$

# Shape optimization

We first note the homothety property of the Steklov-Helmholtz spectrum:

[see lemma](#)[see example](#)

$$\sigma_k(a\Omega, \mu) = \frac{\sigma_k(\Omega, a\mu)}{a}.$$

Problem: *minimize  $|M|\sigma_k$  or  $|\sqrt{\Omega}| \sigma_k$ .*

# Shape optimization

We first note the homothety property of the Steklov-Helmholtz spectrum:

[see lemma](#)

[see example](#)

$$\sigma_k(a\Omega, \mu) = \frac{\sigma_k(\Omega, a\mu)}{a}.$$

Problem: *minimize  $|M|\sigma_k$  or  $|\sqrt{\Omega}| \sigma_k$ .*

Consider  $\Omega_t = \Omega + tv$  and the variational form

$$\sigma_k = \frac{\int_{\Omega} |\nabla u|^2 dx - \mu^2 \int_{\Omega} |u|^2 dx}{\int_M |u|^2 ds},$$

where  $u$  is the  $k$ th normalized eigenfunction with  $\int_M |u|^2 ds = 1$ .

# Shape optimization

We first note the homothety property of the Steklov-Helmholtz spectrum:

[see lemma](#)
[see example](#)

$$\sigma_k(a\Omega, \mu) = \frac{\sigma_k(\Omega, a\mu)}{a}.$$

Problem: *minimize  $|M|\sigma_k$  or  $|\sqrt{\Omega}| \sigma_k$ .*

Consider  $\Omega_t = \Omega + tv$  and the variational form

$$\sigma_k = \frac{\int_{\Omega} |\nabla u|^2 dx - \mu^2 \int_{\Omega} |u|^2 dx}{\int_M |u|^2 ds},$$

where  $u$  is the  $k$ th normalized eigenfunction with  $\int_M |u|^2 ds = 1$ .

Using shape derivatives  $(\cdot)'$  with respect to  $t$  (*time*) (chap. 9 (Delfour et al., 2011)) we get  $(|M|\sigma_k)'$  and  $(|\sqrt{\Omega}| \sigma_k)'$ . [see form](#)

# Shape optimization

We first note the homothety property of the Steklov-Helmholtz spectrum:

[see lemma](#)
[see example](#)

$$\sigma_k(a\Omega, \mu) = \frac{\sigma_k(\Omega, a\mu)}{a}.$$

Problem: *minimize  $|M|\sigma_k$  or  $|\sqrt{\Omega}| \sigma_k$ .*

Consider  $\Omega_t = \Omega + tv$  and the variational form

$$\sigma_k = \frac{\int_{\Omega} |\nabla u|^2 dx - \mu^2 \int_{\Omega} |u|^2 dx}{\int_M |u|^2 ds},$$

where  $u$  is the  $k$ th normalized eigenfunction with  $\int_M |u|^2 ds = 1$ .

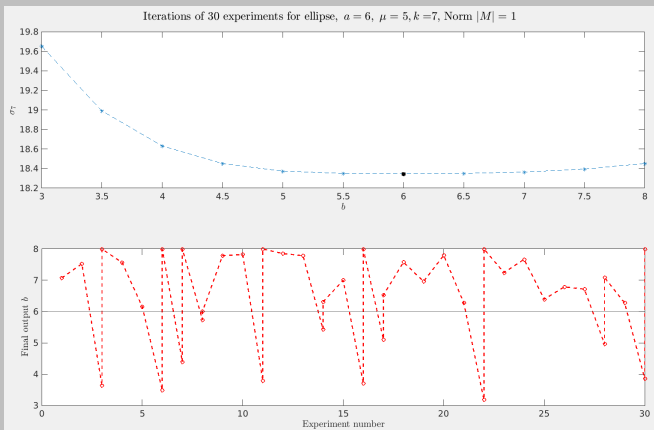
Using shape derivatives  $(\cdot)'$  with respect to  $t$  (*time*) (chap. 9 (Delfour et al., 2011)) we get  $(|M|\sigma_k)'$  and  $(|\sqrt{\Omega}| \sigma_k)'$ . [see form](#)

Through experiments we observe that the optimization for  $|M|\sigma_k$  ( $|\sqrt{\Omega}| \sigma_k$ ) runs into a Dirichlet-Laplace eigenvalue.

# Shape optimization with fixed perimeter I

Problem: *minimize  $\sigma_k$  with  $|M| = 1$ .*

For the ellipse  $\frac{x^2}{6^2} + \frac{y^2}{b^2} = 1$ , we consider  $b \in [3, 8]$ . The smallest  $\sigma_7$  is for  $b = a$ .  
Only 1/30 experiments converge here.



## Shape optimization with fixed perimeter II

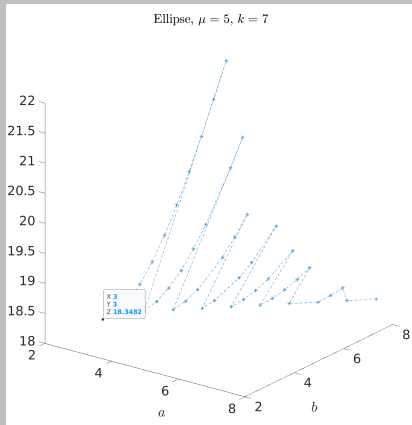
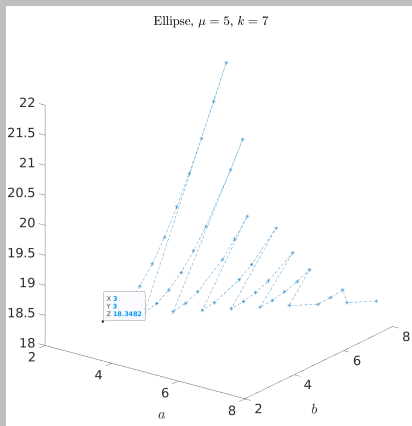


Figure 15:  $\sigma_7$  for various ellipses,  
 $|M| = 1$ .

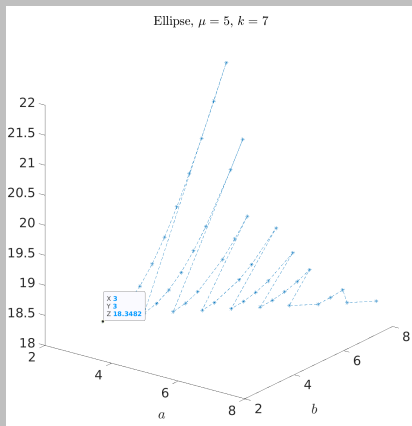
## Shape optimization with fixed perimeter II



- For the ellipse  $\frac{x^2}{a^2} + \frac{y^2}{b^2} = 1$ , we consider  $a, b \in [3, 8]$ .
- The smallest eigenvalue occurs when  $a = b$ .

Figure 15:  $\sigma_7$  for various ellipses,  
 $|M| = 1$ .

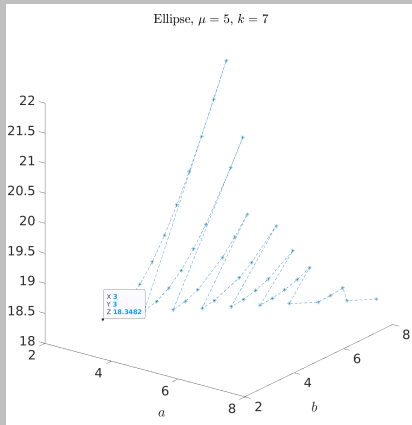
## Shape optimization with fixed perimeter II



- For the ellipse  $\frac{x^2}{a^2} + \frac{y^2}{b^2} = 1$ , we consider  $a, b \in [3, 8]$ .
- The smallest eigenvalue occurs when  $a = b$ .
- 26/30 experiments converge to  $a = b = 8$ .

Figure 15:  $\sigma_7$  for various ellipses,  
 $|M| = 1$ .

## Shape optimization with fixed perimeter II



- For the ellipse  $\frac{x^2}{a^2} + \frac{y^2}{b^2} = 1$ , we consider  $a, b \in [3, 8]$ .
- The smallest eigenvalue occurs when  $a = b$ .
- 26/30 experiments converge to  $a = b = 8$ .
- While this is a correct configuration, it is not the only one.

Figure 15:  $\sigma_7$  for various ellipses,  
 $|M| = 1$ .

## Shape optimization with fixed perimeter II

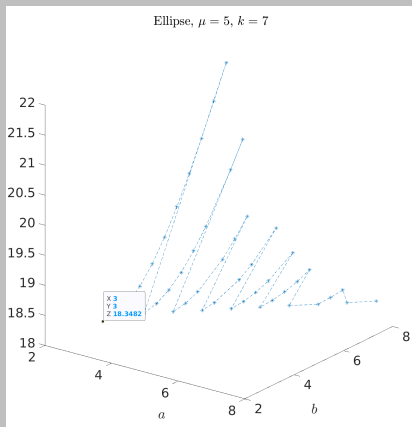


Figure 15:  $\sigma_7$  for various ellipses,  
 $|M| = 1$ .

- For the ellipse  $\frac{x^2}{a^2} + \frac{y^2}{b^2} = 1$ , we consider  $a, b \in [3, 8]$ .
- The smallest eigenvalue occurs when  $a = b$ .
- 26/30 experiments converge to  $a = b = 8$ .
- While this is a correct configuration, it is not the only one.
- Further, it is also an endpoint.

## Shape optimization with fixed perimeter II

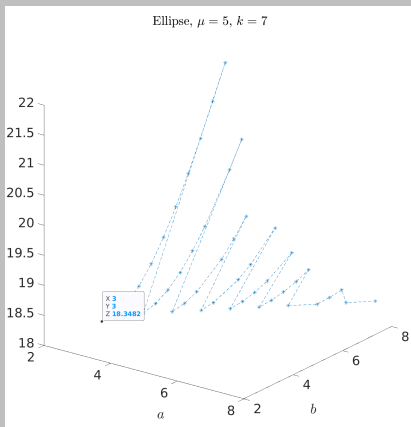


Figure 15:  $\sigma_7$  for various ellipses,  
 $|M| = 1$ .

- For the ellipse  $\frac{x^2}{a^2} + \frac{y^2}{b^2} = 1$ , we consider  $a, b \in [3, 8]$ .
- The smallest eigenvalue occurs when  $a = b$ .
- 26/30 experiments converge to  $a = b = 8$ .
- While this is a correct configuration, it is not the only one.
- Further, it is also an endpoint.
- Maybe algorithm defaults to an endpoint.